J Neurophysiol 97: 248–263, 2007.
First published October 18, 2006; doi:10.1152/jn.01098.2005.

Feedforward Inhibition Controls the Spread of Granule Cell–Induced Purkinje Cell Activity in the Cerebellar Cortex

Fidel Santamaria,[1] Patrick G. Tripp,[3] and James M. Bower[2,3]

[1]*Computation and Neural Systems Program, California Institute of Technology, Pasadena, California;* [2]*Research Imaging Center, University of Texas Health Science Center at San Antonio; and* [3]*Cajal Neuroscience Research Center at the University of Texas San Antonio, San Antonio, Texas*

Submitted 12 October 2006; accepted in final form 13 October 2006

Santamaria F, Tripp PG, Bower JM. Feedforward inhibition controls the spread of granule cell–induced Purkinje cell activity in the cerebellar cortex. *J Neurophysiol* 97: 248–263, 2007. First published online October 18, 2006; doi:10.1152/jn.01098.2005. Synapses associated with the parallel fiber (pf) axons of cerebellar granule cells constitute the largest excitatory input onto Purkinje cells (PCs). Although most theories of cerebellar function assume these synapses produce an excitatory sequential "beamlike" activation of PCs, numerous physiological studies have failed to find such beams. Using a computer model of the cerebellar cortex we predicted that the lack of PCs beams is explained by the concomitant pf activation of feedforward molecular layer inhibition. This prediction was tested, in vivo, by recording PCs sharing a common set of pfs before and after pharmacologically blocking inhibitory inputs. As predicted by the model, pf-induced beams of excitatory PC responses were seen only when inhibition was blocked. Blocking inhibition did not have a significant effect in the excitability of the cerebellar cortex. We conclude that pfs work in concert with feedforward cortical inhibition to regulate the excitability of the PC dendrite without directly influencing PC spiking output. This conclusion requires a significant reassessment of classical interpretations of the functional organization of the cerebellar cortex.

INTRODUCTION

The distinctive orthogonal projection of the parallel fibers (pfs) through Purkinje cells (PCs) in the cerebellar cortex has dominated speculations concerning cerebellar function for more than 100 years (Albus 1971; Anastasio 2001; Braitenberg et al. 1997; Cajal 1904; Hofstotter et al. 2002; Marr 1969; Medina and Mauk 2000; Sultan and Heck 2003; Yamamoto et al. 2002). A fundamental assumption in most of the resulting theories of cerebellar function is that a focal activation of the granule cell layer produces a sequential activation of PCs along the course of the pfs. The primary physiological support for this assumption, known as the *beam hypothesis* (Braitenberg and Atwood 1958), has come from studies in which pf activity is induced with direct electrical stimulation of the molecular layer (Coutinho et al. 2004; Dunbar et al. 2004; Eccles et al. 1966a; Gao et al. 2003; Ito and Kano 1982). However, numerous efforts to obtain beams of PCs under more natural forms of activation of the granule cell–pf–PC pathway have failed (Bell and Grimm 1969; Bower and Woolston 1983; Cohen and Yarom 1998; Eccles et al. 1972; Kolb et al. 1997). Instead, the subset of these studies that have recorded from both granule cell and PC layer activity demonstrated that activated PCs are found only immediately overlying stimulated regions of the granule cell layer (Bower and Woolston 1983; Cohen and Yarom 1998; Jaeger 2003; Kolb et al. 1997; Lu et al. 2005), leaving the influence of pfs unresolved (Bower 2002).

The lack of clear pf beamlike effects in vivo from an input that, in mammals, provides approximately 150,000 excitatory synapses per PC (Gundappa-Sulur et al. 1999; Harvey and Napper 1991) has posed a physiological conundrum for almost 50 years (for review see Bower 2002). All published explanations for the lack of beamlike effects under more natural stimulus conditions have proposed that pfs are less powerful than previously believed (Eccles et al. 1972), either because of the desynchronization of action potentials as they travel along the pfs (Llinás 1982) or because of the small number of simultaneously activated granule cells (Braitenberg et al. 1997).

We first used a computer model of the cerebellar cortex to test these previous explanations. We found that even when the maximum likely pf desynchronization was combined with a very small number of activated granule cells, the model produced a full beam of activated PCs. However, when molecular layer inhibition was added to an otherwise identical network model, beamlike pf effects did not occur, suggesting that molecular layer inhibition is responsible for the lack of beamlike activation of PCs under natural stimulus conditions in vivo. To test this most fundamental prediction of the model, we recorded tactile evoked responses in PCs in vivo located along the pfs in the presence and absence of two different γ-aminobutyric acid type A ($GABA_A$) receptor blockers (bicuculline and gabazine). As the model predicted, blocking molecular layer inhibition with either drug resulted in the emergence of beamlike patterns of PC activity consistent with stimulation by pf synapses.

After experimentally testing the model prediction, we completed a more detailed analysis of our modeling results, producing several more specific predictions for the inhibitory mechanisms underlying the ability of feedforward inhibition to counterbalance pf excitation. These results will serve as the basis for future experimental and modeling studies and also have important implications for theories of cerebellar function in general and the role of pfs in particular.

METHODS

Modeling procedures

MODEL STRUCTURE. *Purkinje cell.* We used our previously published PC model (De Schutter and Bower 1994a,b) with updated

Address for reprint requests and other correspondence: J. M. Bower, Research Imaging Center, University of Texas Health Science Center at San Antonio, 7703 Floyd Curl Drive, San Antonio, TX 78284-6240 (E-mail: bower@uthscsa.edu).

The costs of publication of this article were defrayed in part by the payment of page charges. The article must therefore be hereby marked "*advertisement*" in accordance with 18 U.S.C. Section 1734 solely to indicate this fact.

synaptic kinetics. The ion channels, their kinetics, and distributions are described in detail in the Supplementary Material Table S1.

Granule cells. Granule cells were distributed in a 300 × 2,500-μm area, 20 μm below the PC somas. Each cell gave rise to an axon that coursed vertically into the molecular layer (ascending segment), making a synaptic contact with the overlying PC every 10–90 μm (Gundappa-Sulur et al. 1999; Harvey and Napper 1991). After ascending for varying distances through the molecular layer, the granule cell axon bifurcates into a pf (Fig. 1*A*).

Propagation velocities of action potentials along pfs varied linearly from the bottom to the top of the molecular layer, with the fastest at the bottom and the slowest at the top (Vranesic et al. 1994). To account for natural variations in the depth and shape of the granule cell layer, homogeneous noise was added to pf conduction velocities in a range of 0 to 40% base values. In the absence of evidence to the contrary, we assumed that the ascending segments have the same propagation velocities as their associated pfs. The kinetics of all excitatory synapses are described in the Supplementary Materials Table S2.

Molecular layer interneurons. The biophysical properties of these cells were not represented explicitly, but instead their influence was parameterized by the activation of their synapses on PCs. Molecular interneurons make two types of synapses on PCs: stellate-type connections on dendrites and basket-type connections on the PC soma (Sultan and Bower 1988). The type and number of these connections are dependent on the depth of the interneuron's soma in the molecular layer: the deeper the soma the more basket-type synapses it produces (Sultan and Bower 1998). Reflecting these anatomical constraints, the PC's dendritic tree was divided into three horizontal overlapping layers: from −100 to 200, 100 to 300, and 200 to 400 μm, where 0 is the position of the soma (Fig. 1*B*). Synapses in the top layer made only stellate-type connections, whereas cells in the middle and bottom layers made both stellate- and basket-type connections, with the bottom layer biased toward basket-type synapses. Stellate- and basket-type synaptic kinetics are described in Supplementary Material Table S2.

MODEL ACTIVATION. *Background excitatory and inhibitory activity.* We implemented 1,600 granule cells (and the same number of passive spines on the PC), which corresponds to roughly 1% of the total granule cell input believed to converge onto an average PC (Harvey and Napper 1991). We compensated for this reduction in the number of inputs by increasing the firing rate of these synapses (De Schutter and Bower 1994c) with the updated synaptic kinetics (Supplementary Material Figure S1). The number of modeled inhibitory inputs contacting the PC dendrite in these simulations was 1,695, which anatomical data suggest is close to a realistic value (Sultan and Bower 1998).

Unless otherwise noted the background activation of the granule cells and inhibitory synapses was modeled as a Poisson process with a mean firing rate of 4.0 Hz for granule cells and 1.1 Hz for inhibitory synapses. This background stimulation reproduced the average 40-Hz PC firing rate found in vivo (Bower and Woolston 1983). Because the random background pf and inhibitory inputs were assumed to arise from spontaneous granule cell layer activity from throughout the cerebellum folium, we did not correlate these inputs in the model. As described later, however, stimulus-evoked activity in the pfs and molecular layer interneuron was correlated through the appropriate network connections.

Focal granule cell layer activation. Reflecting the patchy organization of mossy fiber tactile inputs (Shambes et al. 1978) as well as the width of our PC model dendrite, a focal activation of the granule cell layer was modeled by synchronously activating a nearly 300-μm-wide section of the granule cell layer with variable length. The ascending and pf synapses associated with the granule cells in this patch were activated after the temporal delay resulting from the propagation velocity of the axon and the distance from the site of activation. We opted for a synchronous activation of all granule cells instead of a temporally spread function to rigorously test the desynchronization hypothesis. Any temporal spread in activation of the granule cells would increase the level of desynchronization along the pfs, resulting in a relaxing of the conditions for setting up compensatory feedforward inhibitory inputs on PCs (see RESULTS).

An upper value for the maximum number of activated granule cells was estimated based on data obtained from micromapping tactile responses in the cerebellar granule cell layer (Bower and Kassel 1990; Shambes et al. 1978). Specifically, a single upper lip tactile stimulus to the ipsilateral rat face consistently activates a 500 × 500-μm cortical area in the center of folium Crus IIa (Fig. 4). Using published values for the average concentration of granule cells (Harvey and Napper 1991) and taking into account the 300-μm width of the modeled PC dendritic tree, we estimated that an upper lip tactile stimulus results in at most 30,000 active granule cell synapses per PC. For the pfs, this value corresponds to 20% of the total 150,000 pf excitatory inputs per PC.

Pf activation of molecular layer interneurons. Activation of feedforward inhibitory synapses was implemented as a variable delay after pf activity. In each of the three subdivisions of the molecular layer (see above) a variable subset of inhibitory synapses was randomly selected to be activated by the first arriving pf input. The synapses were activated over a range of time with a minimum value of 1 ms to account for the reaction time of the molecular layer interneuron dendrite, the cell's firing threshold, and the interneuron axonal propagation delay. In the case of basket-type synapses originating in the middle layer, an additional delay was added to account for the additional axonal propagation to the PC layer.

A summary of all network parameters is shown in Supplementary Material Table S2.

DATA ANALYSIS. Peristimulus time histograms (PSTHs, 1-ms bin) were constructed from PC spike times 10 ms before and 20 ms after simulated stimulus onset. The significance of changes in the shape of the PSTH, poststimulus, was quantified using *t*-test, dividing the total number of trials (128 or 256) in subsets of 16 (Santamaria and Bower 2005; Santamaria et al. 2002) and comparing the firing rates of the PC before and after the stimulus. The pattern of background excitatory and inhibitory synaptic inputs was randomized on each trial and was therefore completely independent of the pattern of stimulus-evoked excitatory and inhibitory input.

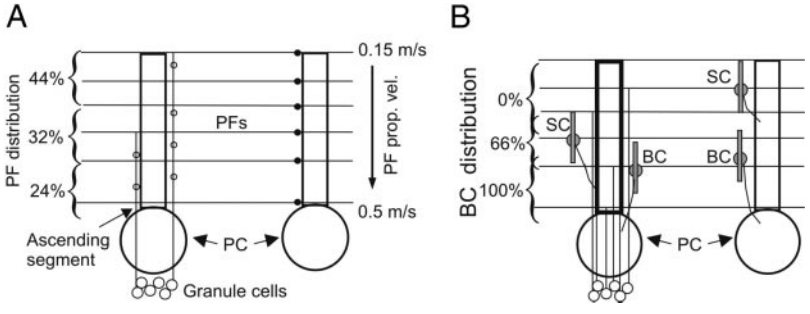

FIG. 1. Cerebellar cortex network model. *A*: distribution of granule cell synapses on a PC located above an activated region of granule cell layer (*left*) and at a distance (*right*). There are 2 types of granule cell synapses: ascending segment (○) and parallel fiber (●). *B*: distribution of molecular interneuron synapses on Purkinje cells (PCs). Dendritic trees of the PCs were divided in 3 overlapping layers onto which inhibitory synapses from stellate cells (SCs) and basket cells (BCs) were differentially distributed.

Simulations for each set of data were performed using a fixed range for pf propagation velocities and fixed numbers of activated granule cells. Systematic parameter variations were made until the model produced PSTHs that came closest to matching previous experimental results.

To avoid any biases introduced by the particular spatial distribution of inputs, the physical positions of all the synaptic inputs on PC dendrites were randomized from trial to trial. All simulations were implemented in GENESIS 2.1 (Bower and Beeman 1995) running on supercomputers operated by the San Diego Super Computer Center at the University of California, San Diego.

Experimental procedures

Modeling predictions were tested, in vivo, using fourteen 3- to 6-mo-old female Sprague–Dawley rats. Animal handling, surgical procedures, and euthanasia techniques were approved by the Caltech Animal Care and Use Committee as well as the Animal Use Committee at the University of Texas Health Science Center in San Antonio as in compliance with the National Institutes of Health guidelines. Details of surgical procedures and recording techniques can be found in the Supplementary Materials. All recordings were obtained in animals anesthetized using ketamine–xylazine–acepromazine (ketamine 100 mg/kg; xylazine 5 mg/kg; acepromazine 1 mg/kg). This combination of drugs results in granule cell layer responses most similar to those obtained in awake behaving animals (cf. Fig. 2, *trace 2*; Hartmann and Bower 2001).

Unitary PC responses were recorded along the mediolateral axis of Crus IIa, which is the same axis along which the pfs course (Bower and Woolston 1983). PCs were identified by their depth in the molecular layer, firing frequencies, and the presence of both simple and complex spontaneous spiking activity (Simpson et al. 1996). The tactile receptive fields of the granule cell layer were mapped after several experiments to reconfirm the distribution of sensory inputs within the folium (Bower and Kassel 1990). Tactile stimuli were delivered under computer control using a solenoid-activated rod with a 1-mm^2 tip placed to contact different perioral regions. A typical data collection trial consisted of 240 stimuli presented at 1.0 Hz. In some experiments, multiple PCs were recorded simultaneously along the pfs using a multiunit recording system designed and built based on tungsten electrodes. Electrode impedances (MPI, Federalsburg, MD) were 4 or 10 MΩ for PCs and 2 to 4 MΩ for recording of the granule cell layer.

PCs responses were recorded before and after topical application of either $GABA_A$ receptor blocker bicuculline or gabazine (SR95531), all obtained from Sigma. These drugs were applied using a micropositioner to place a 10-μl microsyringe (Hamilton) within several microns of the surface of the cerebellum. Between 1 and 7 μl of either a 5 mM saline solution of bicuculline or 60 μM gabazine were applied to the surface of the cerebellum, forming a small bubble that spread over the surface, covering the position of all recording electrodes. Data collection was resumed 10–15 min after drug application. Multiunit recordings of granule cell layer activity were also recorded before and after inhibitory blockers were applied. Data analyses are reported as SE unless otherwise noted. Changes in PC activity recorded experimentally were quantified using the same statistical procedure as that for the modeled data (see above).

RESULTS

Simulated spatiotemporal patterns of granule cell axon activity

Our initial objective was to use the computer model to test the hypothesis that either the desynchronization of action potentials traveling along pfs (Llinás 1982) or an insufficient number of simultaneously activated granule cells (Braitenberg et al. 1997) is responsible for the lack of PC beams seen in vivo under natural stimulus conditions (Bower and Woolston 1983; Kolb et al. 1997).

To determine the largest likely level of pf desynchronization, we first used the model to estimate the spatial and temporal spread of action potentials along pfs after a focal activation of the granule cell layer. Figure 2*A* shows the spatial distribution of action potentials in the molecular layer calculated using the widest difference in conduction velocities reported in mammals between superficial (0.15 m/s in rats; Vranesic et al. 1994) and deep pfs (0.5 m/s in cats; Crepel et al. 1981). Figure 2*A* shows that with these values, an originally synchronous volley of action potentials would spread over >1.5 mm of the molecular layer by the time the fastest action potentials reached the end of the pfs (2.5 mm; Harvey and Napper 1991). Note that we chose the widest reported mammalian values to provide the best possible conditions for the desynchronization hypothesis. A narrowing or lack of difference in superficial and deep pf conduction velocities would reduce the level of action potential desynchronization and generate more stringent conditions for this hypothesis. Also, whereas this graph was made assuming depth-related differences in pf conduction velocities, the lag in propagation of pf action potentials in the superficial layers of the molecular layer also occurs as a consequence of action potentials propagating along the full length of the ascending granule cell axon segment and the spatial distribution of the granule cells.

Figure 2*B* shows the distribution of the predicted propagation times for pf action potentials converging on PCs at different distances from a focal site of granule cell layer activation. The shortest propagation time (lower bound) is a combination of the fastest propagation velocity with travel along the deepest pfs. Similarly, the upper bound is the prop-

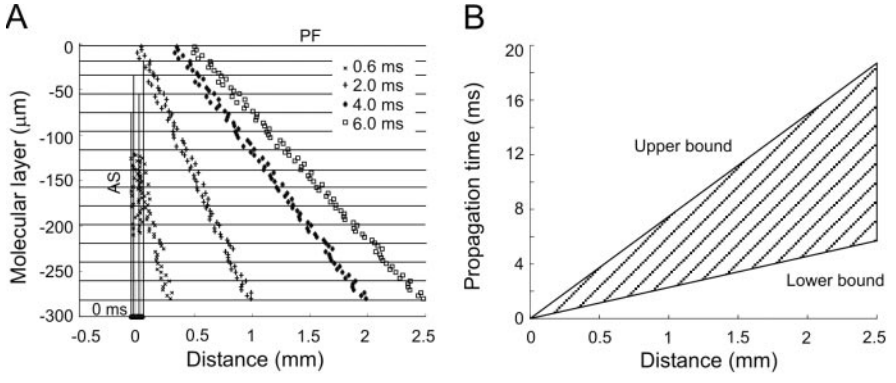

FIG. 2. Spatial and temporal patterns of action potential propagation along granule cell axons. *A*: a synchronously activated patch of granule cells, consisting of 80 cells distributed over 50 μm^2 along the *x*-axis, resulted in an increasingly desynchronized volley of parallel fiber (pf) activity over time arising from both the time to reach the axon bifurcation point and the different propagation velocities at different depths in the molecular layer. *B*: range of propagation times for action potentials converging at different distances from the site of granule cell activation. Upper and lower bounds are calculated using the slowest (0.15 m/s) and fastest (0.50 m/s) propagation velocities of pf action potentials.

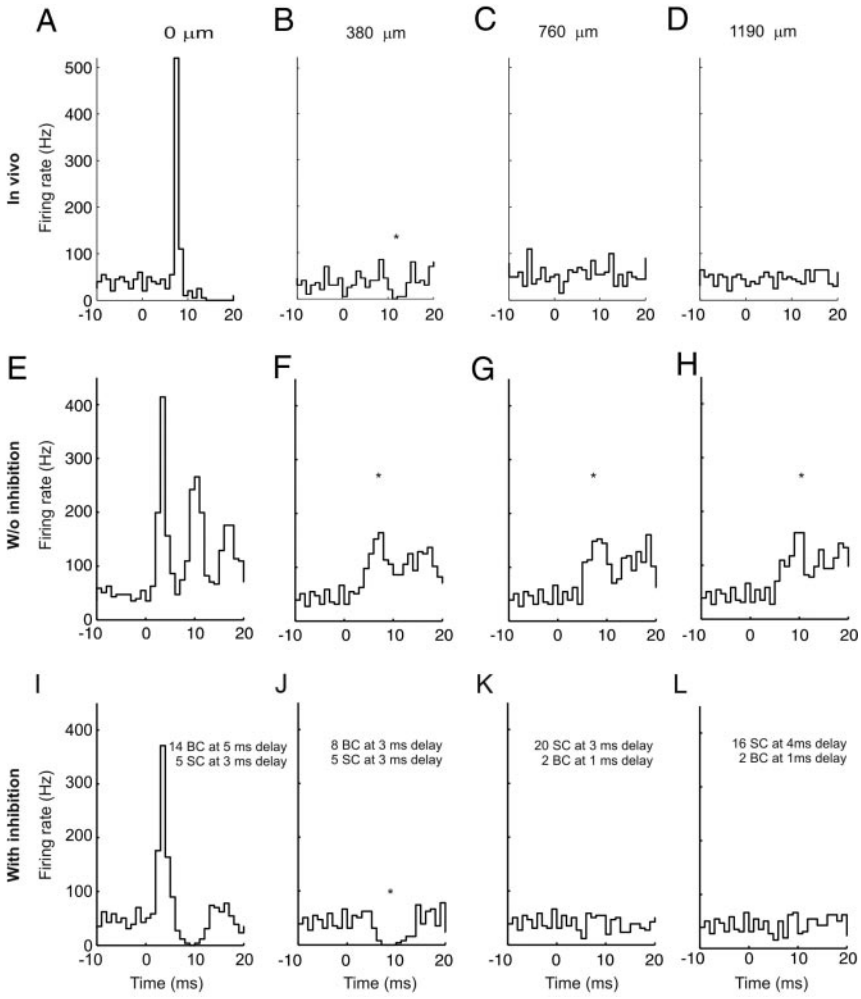

FIG. 3. Experimental and modeled granule cell effects on PCs. *A–D*: peristimulus time histograms (PSTHs, 300 trials) of simultaneously recorded PCs evoked by tactile stimulation of the ipsilateral upper lip in vivo. *A*: PC immediately above the stimulated region of granule cells. *B–D*: PCs recorded along the path of the pfs at the indicated distances. *E–H*: PSTHs (256 trials) from network simulations using the largest range of pf conduction velocities (0.15 top, 0.5 m/s bottom), and 4% of granule cells activated. *I–L*: similar simulations as *E–H* with feedforward inhibition added to the model. *E* and *I* received the same total amount of excitatory input, split between ascending and pf synapses. Notations indicate the inhibitory conduction delays as well as the number of BC and SC synapses converging on the corresponding PCs. All simulated PCs in this and subsequent figures received randomly activated excitatory and inhibitory synapses resulting in an average spontaneous firing frequency of 40 Hz. Difference in the delay in the excitatory onset latency in the in vivo (*A*) and modeled (*E* and *I*) PCs is attributed to the additional conduction delays from the stimulated skin to the cerebellum in vivo that, for simplicity, were not included in the model. * denotes statistically significant difference from background activity (*t*-test, $P < 0.05$).

agation time along the most superficial pfs. Because the model assumes that pf propagation velocities vary linearly with respect to their laminar position in the molecular layer the difference between the upper and lower bounds indicates the maximum synaptic desynchronization for PCs located at different distances from a focal site of granule cell layer activation. Accordingly, for a PC 1 mm away from the site of stimulation, the maximum synaptic desynchronization is 4 ms whereas for a PC at 2.5 mm, it is 13 ms.

Simulated PC responses to granule cell activity

The *top two rows* of PSTHs in Fig. 3 compare the typical spatial distribution of PC responses along the path of pfs recorded in vivo after a focal activation of the granule cell layer (Fig. 3, *A–D*) with responses obtained in the model under maximum conditions of pf desynchronization (Fig. 3, *E–H*). The in vivo data shown in Fig. 3, *A–D* were obtained from four PCs recorded simultaneously at the distances shown from the site of focal granule cell layer activation. The PCs were recorded in a mediolateral line down the center of the crown of Crus IIa and therefore along the course of the pfs. In agreement with previous reports (Bower and Woolston 1983; Kolb et al. 1997), the only PC that responds with short-latency excitation is located immediately above the activated region of the granule cell layer (at 0 μm). PCs farther away from the site of granule cell layer activation, and along the course of the pfs, respond at a short distance with a reduction in spiking frequencies and at greater distances with no significant change in firing rate.

The PSTHs shown in Fig. 3, *E–H* were generated by applying the pf desynchronization values shown in Fig. 2*B* to simulated PCs located at the same distances from a focal activation of the granule cell layer as in the experimental data (Fig. 3, *A–D*). The responses shown were obtained from simulation trials in which only 4% of the modeled granule cells were activated. Thus in this example, we combined the largest likely degree of pf desynchronization with a very small number of activated granule cells (and therefore pfs). Nevertheless, it is apparent that the resulting pf input is fully capable of generating beamlike excitatory responses in PCs in the model, producing short-latency excitatory responses even in PCs located 2 mm from the site of granule cell layer activation. The arrival of pfs at this distance is spread out over 11 ms. The progressive shift in latency of the PSTHs reflects the mean propagation velocity of the volley of action potentials along the pfs (0.3 m/s).

The generation of propagating beams of PC activity in the model was robust to a wide range of parameter values. For example, beams of PCs were found even when as little as 2% of the simulated granule cells were activated. Further, the

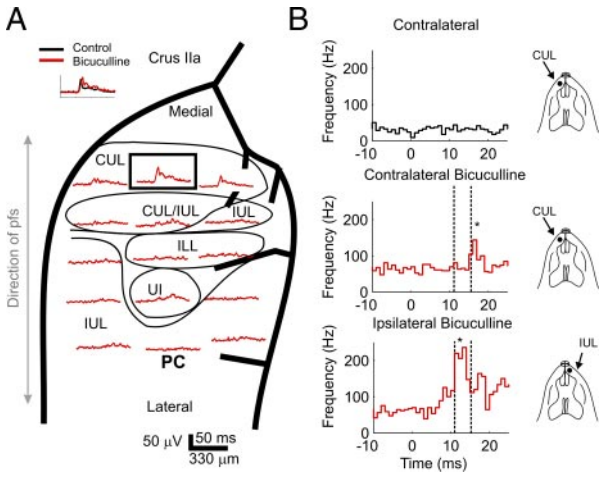

FIG. 4. Bicuculline application results in beams of pf activated PCs. *A*: schematic of folium Crus IIa from which all data in the figure were obtained. Distribution of tactile receptive fields is indicated by the solid lines. Averaged and rectified responses to contralateral upper lip (CUL) stimulation are shown centered on the positions from which they were recorded. Traces in the *top left* compare pre- (black) with post- (red) bicuculline granule cell responses obtained in the location highlighted by the bold rectangle. *B*: PSTHs (240 trials) of a PC before and after bicuculline application recorded at site marked "PC" in *A*. *Top*: response to CUL stimulation before bicuculline application. *Middle* and *bottom*: response to CUL and IUL stimulation, respectively, after bicuculline application. Dashed lines compare the timing of these 2 responses. *Insets*: receptive fields stimulated in each case. IUL, ipsilateral upper lip; ILL, ipsilateral lower lip; UI, upper incisor. * denotes statistically significant difference from background activity (*t*-test, $P < 0.05$).

results were independent of parameters related to the background levels of excitatory and inhibitory inputs (Supplementary Material Figure S1). Thus our modeling results suggest that under a broad range of parameters, even a highly desynchronized parallel fiber volley with a small number of action potentials is more than capable of inducing beamlike activation of PCs. Clearly, however, the simulations do not match the in vivo experimental results, strongly suggesting that some factor other than pf action potential desynchronization or the number of activated granule cells is responsible for the lack of PC beams in vivo.

Simulated effects of feedforward inhibition on PC responses to granule cell activity

The only stimulus-evoked synaptic inputs to PCs in the modeling results presented to this point were provided by excitatory granule cell synapses. However, pfs also synapse directly on molecular layer interneurons, which themselves provide an inhibitory feedforward inhibition on PCs (Cajal 1904; Eccles et al. 1966a). The PSTHs shown in Fig. 3, *I–L* were obtained from simulations identical to those used for Fig. 3, *E–H*, after adding feedforward molecular layer inhibition of both the basket- and stellate-types to the model. By tuning values for the delay only between pf excitation to PC inhibition, the total number of activated inhibitory synapses, and their spatial distribution, the model readily reproduced the short-latency excitation directly above the activated granule cell layer (Fig. 3*I*), the reduction in firing frequency at slightly longer latencies in overlying and nearby PCs (Fig. 3, *I* and *J*), and the lack of PC responses at a distance along the pfs (Fig. 3, *K* and *L*), all also seen in the in vivo data (Fig. 3, *A–D*). Similar results were obtained over a wide and robust range of model parameters (see Fig. 6), including a much narrower range of pf propagation velocities (0.20–0.27 m/s; Supplementary Materials Figures S1 and S2). As described in the final section of the RESULTS, all values for molecular layer inhibition were also within likely physiological values. The model therefore predicts that the lack of PC beams in vivo, after focal activation of the granule cell layer, is a consequence of the presence of feedforward molecular layer inhibition.

In vivo feedforward inhibition controls PC responses to granule cell activity

To test the prediction that the lack of pf activated beams of PCs is attributed to the influence of molecular layer inhibitory interneurons we extracellularly recorded granule and PC activity before and after topical application of two different $GABA_A$ receptor blockers: bicuculline (Fig. 4) and gabazine (Fig. 5). As in previous studies (Bower and Woolston 1983; Lu et al. 2005), we took advantage of the known fractured somatotopy of afferent tactile projections to the cerebellar folium Crus IIa, in which small areas of the granule cell layer receive tactile input from distinctly different perioral regions (Bower and Kassel 1990).

Figure 4 shows representative results when blocking inhibition with bicuculline. All the data shown are from a single experiment, with Fig. 4*A* indicating the distribution of granule cell layer responses to tactile stimulation in Crus IIa. Granule cell layer receptive field mapping procedures (Bower and Kassel 1990) confirmed that medial regions of this folium (closer to the vermis) respond to contralateral upper lip (CUL) stimulation, whereas more lateral regions receive tactile projections from the ipsilateral perioral regions, with a large central representation of the ipsilateral upper lip (IUL). Overlaying this diagram we plotted the averaged and rectified multiunit recordings obtained in the corresponding granule cell layer location after CUL stimulation. Reflecting the receptive field mapping, the granule cell layer is active only in the area representing the CUL and shows no activity within the IUL region. The receptive field mapping was performed before the application of bicuculline, whereas the traces shown here were obtained 17 min after topical application of 5 μl of bicuculline. This indicates that bicuculline does not affect the spatial distribution of tactile-induced granule cell layer activity in Crus IIa. The *top left traces* in Fig. 4*A* compare granule cell layer responses before and after the application of bicuculline for the medial CUL recording site indicated by the bold box.

During the same experiment we recorded the activity of a PC located 1,400 μm lateral to the site of maximum recorded granule cell layer activation. Figure 4*B* shows the calculated PSTHs (240 trials) for this cell during three different experimental conditions. The *top histogram* shows a recording obtained before the application of bicuculline, in which there is no statistically significant response to CUL stimulation. This lack of response is expected because this cell overlies a region of the granule cell layer that does not itself respond to stimulation of the CUL (Fig. 3, *C* and *D*; see Bower and Woolston 1983). In contrast, the *middle histogram* obtained 10 min after bicuculline application shows a strong excitatory response with an onset at 17 ms. If this postbicuculline CUL response arises from pfs, we would expect a longer-latency PC response to

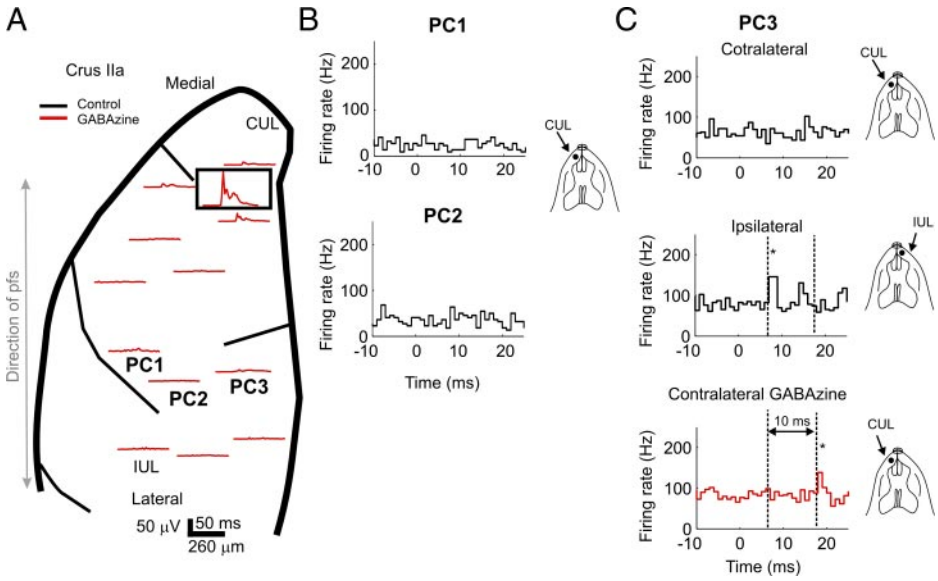

FIG. 5. Gabazine application results in beams of pf-activated PCs. *A*: schematic of folium Crus IIa overlaid with the response of the granule cell layer to stimulation of the contralateral upper lip (CUL) after gabazine application. *B*: PSTHs for PCs recorded in *A* (PC1 and PC2) before gabazine. *C*: PSTHs of PC in location PC3 (in *A*) obtained in response to CUL (*top*) and IUL (*middle*) stimulation before gabazine application. *Bottom*: PSTH recorded 10 min after application of the drug. Dashed lines indicate the timing relationships between the excitatory responses. *Insets*: stimulated receptive field in each case. All PSTHs calculated from 240 trials. Abbreviations as in Fig. 4. * denotes statistically significant difference from background activity (*t*-test, $P < 0.05$).

stimulation of the CUL than the IUL represented in the immediately underlying granule cell layer. The *bottom histogram* in Fig. 4*B* confirms this prediction, showing that IUL stimulation results in a peak excitatory response at 12 ms. The 5-ms difference in the delay of onset between the two responses predicts a putative pf propagation velocity of 0.28 m/s, which is within the reported physiological range (Vranesic et al. 1994).

Figure 5 shows the results of a similar experiment using the more specific $GABA_A$ receptor blocker gabazine (60 μM). Figure 5*A* shows the diagram of Crus IIa for this experiment with overlaid averaged granule cell layer responses to CUL stimulation. The responses were recorded after 5 μl of gabazine was applied. As in Fig. 4*A*, the response is restricted to the medial regions of the folium even after application of gabazine. Figure 5*B* shows PSTHs for two PCs recorded over the IUL patch before gabazine application (PC1 and PC2). Because these PCs overlie a region of the granule cell layer activated by the IUL, CUL does not evoke an excitatory response in these cells under control conditions. Figure 5*C* shows three PSTHs obtained from another PC recorded 1,200 μm away from the site of stimulation (PC3) to CUL stimulation and IUL before the application of gabazine (*top* and *middle histograms*) and to CUL stimulation after application of the drug (*bottom histogram*). As in the case of bicuculline, this PC responds to CUL stimulation only after $GABA_A$ inhibition is blocked (*bottom histogram*). Based on the difference in the onset of this PC response between IUL and postgabazine CUL stimulation, the calculated pf propagation velocity was 0.12 m/s. In those experiments in which putative pf propagation velocities were calculated, the average value with bicuculline was 0.27 ± 0.02 m/s ($n = 3$), whereas it was 0.21 ± 0.07 m/s with gabazine ($n = 3$).

Figure 6 shows the results from a different experimental procedure specifically intended to both replicate the effects of blocking $GABA_A$ inhibition and also estimate pf conduction velocities. We simultaneously recorded from two PCs separated either by 380 μm (Fig. 6*A*) or 760 μm (Fig. 6*B*) along the course of the pfs before and after bicuculline application. The top two PSTHs in Fig. 6*A* were recorded from a cell overlying

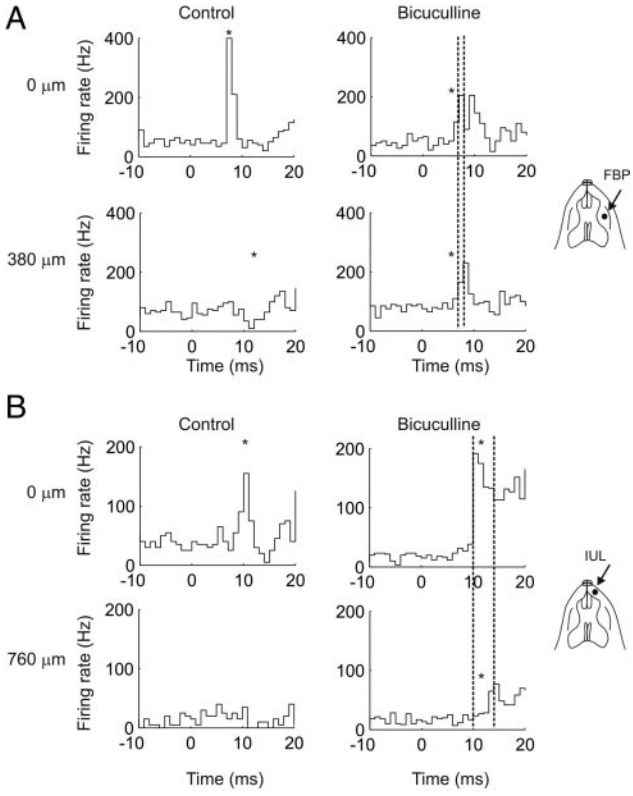

FIG. 6. Estimating pf propagation velocities using simultaneously recorded PCs. *A*: PCs recorded 380 μm away from each other. After stimulation of the furry bucal pad (FBP) the top PC, overlying the activated region of the granule cell layer, responded with a short-latency increase in firing, whereas the bottom PC showed a short latency decrease in firing frequency. After application of bicuculline this PC shows an increase in firing (*bottom right PSTH*) delayed by 1 ms with respect to the time to peak of the PC at 0 μm. *B*: similar experiment as in *A* but with 2 PCs recorded 760 μm apart and stimulation of the IUL. Delay to peak after bicuculline application of the previously unresponsive PC was 5 ms. Each PSTH calculated from 200 trials. *Insets* in each case indicate both the receptive field for the granule cell layer underlying the top PC and the location of the tactile stimulation. * denotes statistically significant difference from background activity (*t*-test, $P < 0.05$).

a region of the granule cell layer that was activated by tactile stimulation of the furry bucal pad (FBP). This cell responds with excitation both before (*left PSTH*) and after (*right PSTH*) topical application of bicuculline. The second PC (*bottom*) was close to but not overlapping the FBP granule cell patch and therefore produced only a short-latency inhibitory response to the same stimulus under control conditions. However, after bicuculline was applied, this cell responded with short-latency excitation. The delay between the onsets of excitation between these two cells is 1 ms, which results in a calculated pf conduction velocity of 0.38 m/s. For all seven pairs of cells recorded with a 380-μm separation, the average calculated pf conduction velocity was 0.26 $\pm$ 0.05 m/s.

Similarly, Fig. 6*B* shows data from two PCs separated by 760 μm after IUL stimulation. The cell located over the IUL granule cell patch again responded with increased firing both before (*left*) and after (*right*) bicuculline application. The second cell (*bottom*) showed no change in spiking under control conditions, but showed an increase after the application of bicuculline. In agreement with a delay resulting from action potentials propagating along the pfs, the difference in time to peak of the PCs separated by 760 μm was greater than that for the PCs separated by 360 μm. The calculated pf conduction velocity was 0.15 m/s. The average conduction velocity for the four pairs of cells recorded at a 760 μm distance was of 0.25 $\pm$ 0.08 m/s. The similarity in calculated pf conduction velocities in all experiments, using either drug, strongly suggests that the excitatory responses that emerge after blocking molecular layer inhibition are a direct result of pf input.

Although conduction along the pfs is the most likely explanation for the emergence of propagating short-latency excitatory PC responses after application of the $GABA_A$-receptor–blocking drugs, we also specifically looked for evidence for any changes in PC excitability. Neither bicuculline nor gabazine resulted in a statistically significant change in basal PC firing rates (Fig. 7, *A* and *B*). For bicuculline, average PC firing rates actually showed a slight, although nonsignificant decrease from 41.6 $\pm$ 4.3 to 33.8 $\pm$ 3.2 Hz (n = 30, eight experiments, t-test). In fact, both increases and decreases in firing frequencies were found for different cells in the same experiment. Similarly, gabazine resulted in a slight average reduction from 40.0 $\pm$ 7.8 to 39.2 $\pm$ 12.0 Hz (n = 5, four experiments, t-test, nonsignificant). Thus we found that blocking $GABA_A$ receptors resulted in no statistically significant change in PC excitability.

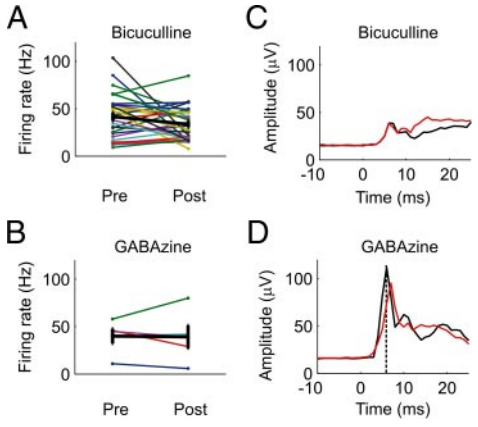

FIG. 7. Blocking γ-aminobutyric acid type A ($GABA_A$) receptors in the cerebellar cortex does not result in an increase in neuronal excitability. *A*: average firing rate for 30 PCs before and after bicuculline application. *B*: average firing rate for 5 PCs recorded before and after gabazine application. *C*: averaged (n = 30 trials) granule cell layer responses obtained from contralateral upper lip (CUL) stimulation before (black) and after (red) bicuculline application. *D*: granule cell layer response from CUL stimulation (n = 30 trials) before and after gabazine application. Error bars in *A* and *B* are for SE.

We also found no significant effect of these drugs on granule cell layer excitability. Figure 7*C* compares representative granule cell layer responses before and after bicuculline application. The basal activity and amplitude of the initial response were unchanged, with a slight increase in the amplitude of the later latency response. This change constituted no more than a 20% increase in the area under the curve during the first 25 ms after the stimulus. On average, the increase in activity was 25 $\pm$ 7% (n = 5). Gabazine had a much smaller average effect (10 $\pm$ 3%, n = 5) and showed no change in many experiments (Fig. 7*D*; plots correspond to the bold box location in Fig. 5*A*). This small influence of gabazine in granule cell response is consistent with previous reports on the weak effect of this drug on the Golgi cell to granule cell synapses (Hamann et al. 2002). We also found no change in the latency of granule cell layer response to either drug (Morissette and Bower 1994).

In summary, neither bicuculline nor gabazine resulted in any significant changes in background PC firing rates, or in the latency, amplitude, or spatial activation of granule cell layer responses to tactile stimulation. Thus the excitatory PC responses at a distance from focal activation of the granule cell layer after blocking inhibition cannot be attributed to a generalized increase in neuronal excitability, but instead is most likely the result of unmasked pf excitation.

Network effects of pf excitation and molecular layer inhibition on PCs

Having experimentally tested the most fundamental prediction of the model, we then explored in more detail the network (Fig. 8) and biophysical (Figs. 9 and 10) interactions underlying the model's ability to replicate in vivo results. Figure 8*A* shows, once again, the range of pf propagation times from the site of origin of granule cell layer activation to a distance of 2 mm. Figure 8*B* shows PC firing rates within 15 ms after the first arrival of action potentials along the pfs for PCs located at different distances from the site of granule cell layer activation. Based on in vivo results (cf. Fig. 3), inhibitory model parameters were chosen so that PCs on top of the site of stimulation increased firing rates by >20% followed by inhibition, whereas PCs between 200 and 400 μm from the site of granule cell layer activation showed a reduction in firing rate of >20%. At greater distances (>400 μm) firing rates of modeled PCs were required to be not statistically different from background ($P < 0.05$).

Figure 8, *C–F* shows the parameter values for feedforward inhibition that produced this pattern of PC activity (see Supplementary Material Table S3 for a summary). Figure 8, *C* and *D* shows spatial variations in the number of basket-type synapses and their temporal delay, whereas Fig. 8, *E* and *F* shows the same analysis for spatial variations in the number and inhibitory delay for stellate-type inhibitory inputs. The shapes and color combinations indicate parameter values corresponding to the same simulation. Overall, the plots show that upper values for inhibitory delays for both basket- and stellate-type

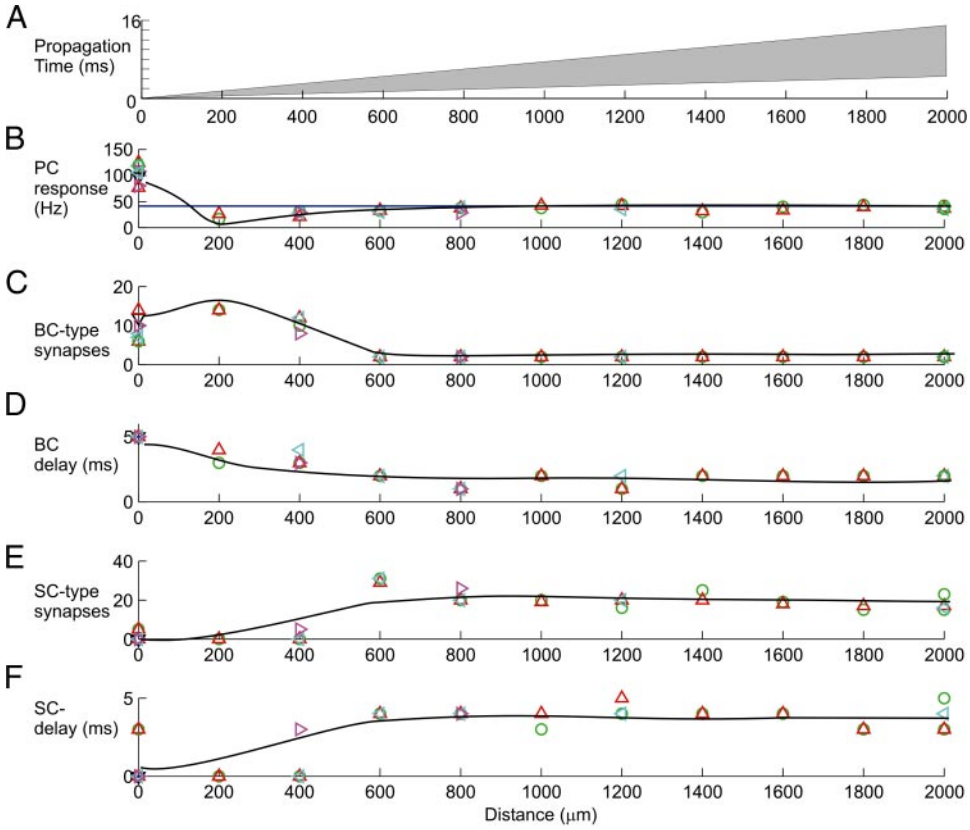

FIG. 8. Spatial and temporal relationships underlying modeled interactions between pf and molecular layer inhibition. *A*: propagation time of the pf volley as a function of distance from the site of granule cell layer activation calculated using the fastest (0.5 m/s) and slowest (0.15 m/s) propagation velocities. *B*: firing frequencies of PCs in a 15-ms window after the first arriving excitatory synaptic input at each distance. *C*: number of basket-type synapses necessary to replicate in vivo physiological data. *D*: range of temporal delays between pf excitation and activation of feedforward basket-type inhibition. *E*: number of inhibitory stellate-type synapses needed to replicate the experimental data. *F*: range of temporal delays between pf excitation and activation of feedforward stellate-type inhibition. Different shaped and colored symbols indicate parameters from the same simulation. Solid lines are interpolations of the mean values at each distance. Each simulation consisted of 256 trials.

synapses ranged from 2 to 5 ms and the strength of either synaptic type ranged from one to 20 synapses.

A fundamental prediction of the analysis presented in Fig. 8, which is a direct result of matching the model to experimental results, is the differential spatial distribution of stellate- and basket-type inhibitory synapses onto PCs (Fig. 8, *C* and *E*). For PCs farther away than 400 μm, suppression of the PC beam was not strongly dependent on the range of inhibitory synaptic delays and was mostly achieved by stellate-type synapses. However, between 0 and 400 μm, pf excitation occurred too quickly (<2 ms) to be compensated for solely by stellate-type inhibition. In this region, accurate simulation of experimental data required basket-type inhibitory inputs. Even then, the ability of this inhibition to shape PC spiking occurred over a fairly wide range of synaptic delays (Fig. 8*D*). Thus our model makes the prediction that the strength of basket- and stellate-type synaptic inhibitions onto PCs is spatially differentiated from the site of granule cell layer stimulation, with basket-type synapses more prominent closer than at greater distances along the pfs.

Biophysical effects of pf excitation and molecular layer inhibition on PC dendrites

The PC spiking output involves a complex interaction between synaptic inputs and the cell's intrinsic electrical and chemical properties (Llinás and Sugimori 1980; Womack and Khodakhah 2002). Modeling studies demonstrated that intrinsic properties produce considerable complexities in the action potential generation process in PCs (De Schutter and Bower 1994c; Etzion and Grossman 1998; Jaeger and Bower 1999; Miyasho et al. 2001; Santamaria and Bower 2005; Watanabe et al. 1998). In this section we focus on the contribution to this discussion provided by interactions between the large intrinsic dendritic currents found in PCs and the relative timing and strengths of excitatory and inhibitory synaptic currents generated by the network model.

Figure 9*A* is a cartoon representation of the timing and spatial relationships between the different excitatory and inhibitory network components of the model. Figure 9, *B–G* shows the average synaptic, dendritic, and dendrosomatic currents, as well as the resulting changes in somatic firing for PCs found above and at three different distances from a focal granule cell layer activation as indicated in Fig. 9*A* ($n = 64$ simulations). The traces shown in Fig. 9, *B–E* are the total summed dendritic currents for each set of channels (Jaeger et al. 1997; see METHODS). Figure 9*B* shows the total granule cell excitatory input in these simulations. This input is provided primarily by ascending segment synapses for the PC at 0 μm and by pf inputs for all other PCs. The steepness of the rise time and the total amplitude of this excitatory input decrease with distance along the pfs as a direct result of the progressive pf desynchronization. Although excitatory synaptic currents have the fastest rise time and largest amplitude for the PC immediately overlying the activated region of the granule cell layer, the induced currents are still large enough even for the most distant PC to generate action potentials in the absence of feedforward inhibition (Fig. 3, *E–H*).

Figure 9, *C* and *D* shows total inhibitory currents generated by stellate- and basket-type synaptic inputs, respectively. As discussed above, replicating the experimental data requires an inverse correlation of the strength of basket- and stellate-type synapses as a function of distance from the site of granule cell

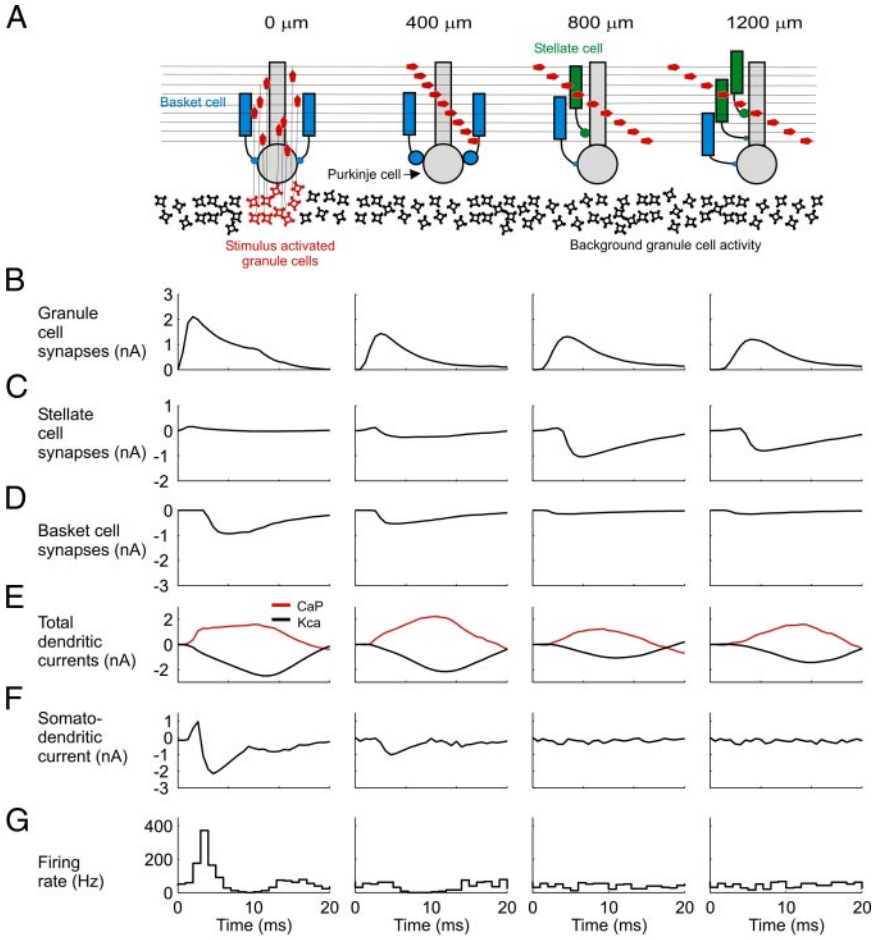

FIG. 9. Biophysical mechanisms underlying excitatory and inhibitory relationships on PCs. *A*: schematic diagram showing synaptic influences on PCs at different distances from the site of granule cell layer activation. Activated granule cells and predicted patterns of pf desynchronization shown in red. Basket- and stellate-type inhibitions represented as blue and green, respectively. *B*: total excitatory currents from granule cell synaptic inputs on PCs. PC at 0 μm received only ascending segment synapses. C: total inhibitory synaptic currents from stellate-type synapses. Although feedforward stellate-type synapses are not activated at 0 and 400 μm the background activated synapses shunt the excitatory depolarization from granule cells. *D*: total basket cell synaptic currents. *E*: total dendritic calcium P currents (CaP, red) and calcium-activated potassium currents (Kca, black) with respect to basal levels of activity after synaptic stimulation. *F*: net somatodendritic current regulating the firing rate of the PC. *G*: PSTH showing the resulting somatic response. All plots correspond to PCs at distances indicated in the schematic diagram at the *top* of the figure. Positive current is inward in *B–E* and toward the soma in *F*. Averages calculated from 64 simulations in *B–E* and 256 in *F*.

layer activation, with basket-type synapses stronger at shorter distances. It should be noted that, even though at short distances (0 and 400 μm) there are no stimulus-activated stellate-type synapses, there is still a net outward flow through the associated channels. This flow arises from current shunting by background-activated stellate-type synapses in response to pf excitatory input that, in effect, results in an immediate damping response to the inward current flowing through these excitatory synapses (Jaeger et al. 1997). The outward flow of current is, of course, bigger at greater distances when stellate-type synapses are actually active.

The large intrinsic voltage-dependent currents in the PC dendrite and soma have a powerful influence on action potential generation (Jaeger et al. 1997). Furthermore, the interaction between dendritic and somatic voltage-dependent conductances is complex (Jaeger and Bower 1999) and its full discussion is beyond the scope of the current paper. However, summed dendritic and somatic currents for these simulations are shown in Fig. 9, *E* and *F*, respectively. In Fig. 9*E*, excitatory granule cell synaptic input results in a local dendritic depolarization that in turn activates dendritic currents, including predominantly CaP (red) and Kca (black) (Santamaria et al.

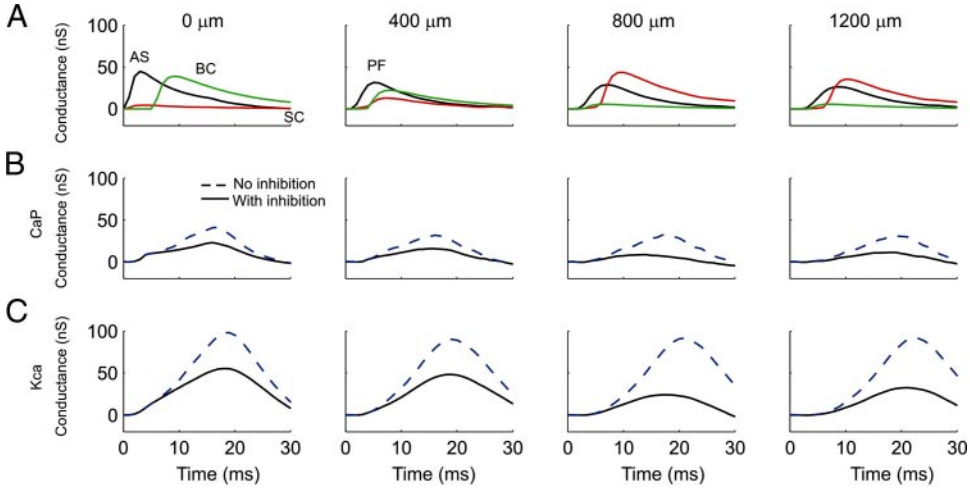

FIG. 10. Synaptic and dendritic conductances in PCs along a pf beam. *A*: granule cell input (black) resulting from ascending segment (AS) synapses at 0 μm and by pfs at longer distances (PF). Inhibitory conductances, from stellate-type (SC, red) and basket-type (BC, green) synapses, account for >90% of the excitatory conductance at 1,200 μm. *B* and *C*: total dendritic conductance for the CaP (*B*) and Kca (*C*) channels in the presence (solid) and absence (dashed) of feedforward inhibition in the model. Number and distribution of inputs were identical to those generating the data in Fig. 9. Averages calculated from 64 simulations.

2002). Ultimately, the influence of these intrinsic currents in the dendritic tree is reflected in the currents flowing between the soma and the dendrite (Fig. 9*F*). This somatodendritic current is then directly reflected in the spiking response of the soma (Fig. 9*G*). For the PC on top of the site of stimulation (0 μm) an initial flow of current from dendrite to soma increases the firing rate at the soma. Activation of basket-type somatic inhibition combined with Kca conductances in the dendrite, however, quickly reverse this current to flow from soma to dendrite, truncating the excitatory spiking response of the PC. For PCs within 400 μm, basket-type inhibition directly on the soma dominates dendrosomatic current flows, resulting in a sharp decrease in PC spiking output even though there is a large excitatory synaptic current in the dendrite (Fig. 9*B*). At greater distances along the pfs, the temporal balance between pf excitatory inputs and stellate-type inhibition at the level of the PC dendritic tree results in a more effective compensation of CaP currents by Kca currents, which in turn results in no net change in the somatodendritic current and therefore no net change in the average firing frequency of the PC. It is important to note, however, that synaptic input in all modeled PCs generates large changes in dendritic currents even when there is no change in average spiking activity in the soma. In fact, the dendritic currents in Fig. 9*E* show that considerably more current generally flows into the dendrite than is actually measured at the soma. The model suggests that the most important issue for PC spiking thus is not the size of synaptic inputs, but the relative timing of the balances between both synaptic (pf and molecular layer interneuron) and intrinsic (CaP and Kca) currents.

The importance for somatic spiking of the timing of activation of dendritic conductances is specifically shown in Fig. 10. The averaged conductance traces ($n = 64$ simulations) associated with granule cell (black) and both basket-type (green) and stellate-type (red) synapses in Fig. 10*A* show that at 0 μm, the short but still finite intrinsic delays in the feedforward inhibitory circuit do not compensate for excitatory input. As activity progresses down the pfs, however, the relative timing of the excitatory and inhibitory (initially basket-type and eventually stellate-type) conductances come more into register, resulting in an almost coincident average onset of excitatory and inhibitory influences even with an intrinsic inhibitory delay (1,200 μm). This somewhat counterintuitive effect is the result of the temporal dispersion of the pf volley and the bottom-to-top progression of the excitatory and thus the inhibitory wave.

As expected, the intrinsic dendritic conductances show a strong dependency on the timing of network effects, which are very sensitive to the presence of inhibition. Figure 10, *B* and *C* compares conductance traces obtained in the presence (solid) and absence (dashed) of feedforward inhibition. Figure 10*B* shows that PCs directly overlying the activated granule cell layer, whether in the presence or absence of feedforward inhibition, generate a substantial CaP conductance, explained by the fact that this conductance is rapidly activated by the excitatory input, rising faster than the time-delayed Kca conductance, and peaking before basket-type inhibitory influences can affect the soma. Figure 10*C* shows a stronger consequence of inhibition in the initial onset of the Kca conductance with a 50% net reduction in peak amplitude. At greater distances along the pfs, however, the increasing desynchronization of the pf input coupled with the counteracting effects of feedforward inhibition are sufficient to generate a slower response of the CaP, allowing its drive on membrane potential to be better compensated for by Kca. In the absence of feedforward inhibition, however, pf input drives a much faster onset in the CaP, reducing the effectiveness of the lagging Kca conductance (see channel kinetics in Supplementary Material Table S1). This is what allows inputs of pfs to directly influence somatic spiking. It is important to note that all these processes regulating the somatodendritic current take place at the level of the dendrite and bear no resemblance to classical synaptic integrative mechanisms that assume a simple summing to threshold of synaptic conductances at the soma.

DISCUSSION

The modeling results presented in this study predict that the lack of pf-generated beams of excited PCs in vivo is attributable to the concomitant pf activation of feedforward molecular layer inhibition. We therefore propose that pf excitation naturally works in concert with molecular layer inhibition to regulate the local voltage dynamics of the PC dendrite and therefore does not contribute to a classic synaptic summing mechanism driving somatic action potential generation. This prediction was supported experimentally by the demonstration that beams of pf-activated PCs emerge in vivo only when molecular layer inhibition is pharmacologically blocked. These results require a significant modification in classical views of functional relationships in cerebellar cortical circuitry as well as cortical function.

Modeling parameters

Desynchronization of action potentials traveling along pfs can come from multiple sources and not only from a linear distribution of propagation velocities as assumed in our study (Vranesic et al. 1994), which has been challenged based on anatomical studies (Wyatt et al. 2005). For example, volleys of action potentials induced by synchronous activation of the granule cell layer would still be desynchronized arising from the fact that deep pfs branch first before the superficial ones in which action potentials travel longer along the ascending segment of the axon. Experimental evidence shows that even direct electrical activation of the pfs results in a rapidly broadening field potential along the pfs, presumably because of variations in pf conduction velocities (Eccles et al. 1966a).

Because there is very little information about the relative timing of molecular layer inhibition and pf excitation, this parameter was lumped and treated as a free variable around which we used parameter-searching techniques to arrive at values producing the best matches to experimental data. With the exception for PCs found overlying or near a focus of granule cell layer activation, the interaction between pf and molecular layer interneurons was robust to synaptic timing. In this case the model suggests that fast somatic basket-type inhibitory input may specifically serve to block pf activation of the PC soma.

Several features of cortical circuitry could potentially affect the timing of inhibition that were not included in the model or are not known, such as molecular layer interneurons coupled by gap junctions (Mann-Metzer and Yarom 1999; van der Giessen et al. 2006) and inhibitory synaptic effects on each

other (Pouzat and Marty 1999). Although gap junctions could contribute to a more rapid spread of inhibitory influence, synaptic interactions could suppress it. We hope that the current study leads to more experimental and modeling interest in the role of molecular layer inhibition in cerebellar processing.

Although we have begun to study the effects of more complex patterns of granule cell layer activation on our models (Santamaria and Bower 2005), in the present work we focused on establishing the conditions under which a pf-driven PC beam was most likely—that is, the synchronous activation of a small region of the granule cell layer. This kind of input produces the most synchronous activation of pfs, maximizing the potential consequences of the additional synaptic delay in the feedforward inhibitory circuitry. Even under these conditions, inhibition was fully capable of counteracting the effect of activation along the pfs. A more gradual and temporally or spatially spread out activation of the granule cell layer can be expected to further reduce the consequences of the additional synaptic delay in the inhibitory pathway. It is worth noting that, experimentally, the more prolonged in vivo granule cell layer responses evoked by peripheral stimulation do not produce beams of activated PCs (Bower and Woolston 1983).

Experimental results

Although it is very easy to remove inhibition from a model, it is more difficult to do so experimentally with precision. We used two different drugs to minimize the likelihood that our results could be attributed to the specific properties of either (e.g., Debarbieux et al. 1998). We showed that normally unresponsive PCs generated an excitatory response in the presence of either bicuculline or gabazine. We also showed that neither drug affects the basal level of PC activity nor the basic timing of either expected or emergent excitatory PC responses. We also demonstrated that these drugs do not affect the spatial organization of tactile inputs to the underlying granule cell layer. However, previous experiments in vivo (Chadderton et al. 2004) and in vitro (Hamann et al. 2002) reported that $GABA_A$-receptor blockers can have an effect on granule cell layer responsiveness, presumably resulting from interference with Golgi cell inhibition. In our data, neither drug affects the onset of the granule cell layer response, but both show a small increase in granule cell layer responsiveness at longer latencies. This result could suggest, for example, that Golgi cell inhibition may more selectively influence secondary activation of the granule cell layer by cortico-cerebellar pathways (Morissette and Bower 1994). It is also possible that the small effects on granule cell layer responsiveness we see arise from the lack of penetration of the drugs from surface application or are a consequence of some other aspect of the granule cell layer–Golgi cell circuitry (Tahon et al. 2005).

Anesthetics are also known to alter the balance between excitation and inhibition (Sonn and Mayevsky 2006; Whittington et al. 2000) and therefore could affect the interpretation of our experimental results. However, the lack of PC beams was previously shown in both anesthetized and unanesthetized preparations (Bower and Woolston 1984; Cohen and Yarom 1998). Furthermore, there is very little difference between the amplitude of granule cell layer responses to tactile stimulation between unanesthetized and ketamine–xylazine-anesthetized rats (compare Fig. 2, *trace 2* with plots in Figs. 4*A*, 5*A*, and 7*D*; Hartmann and Bower 2001). Therefore there is no evidence to suggest that the lack of PC beams is dependent on anesthetic effects.

Although none of the PCs recorded in these experiments showed excitatory responses to distantly activated regions of the granule cell layer under control conditions, not all distant PCs revealed excitatory responses after the application of $GABA_A$-receptor blockers. This lack of response cannot be attributed to GABA-blocker changes in patterns of granule cell layer activity because we specifically controlled for that possibility. However, we previously reported that PCs directly on top of the site of granule cell stimulation were also sometimes unresponsive (Lu et al. 2005). We interpreted this result to suggest that PCs might not be uniform with respect to their responses to granule cell layer activation. This variation in PC responsiveness does not appear to apply to responses to pfs because, again, there is no direct experimental evidence that individual PCs not overlying activated regions of the granule cell layer respond to pf inputs, unless inhibition has been artificially blocked.

Another issue that could be raised with respect to the interpretation of our experimental results is whether some excitatory influence other than the pfs could be responsible for the emergent responses. However, there are numerous reasons to believe that the emergent PC responses arise from pf activity. First, all recorded PCs were located in the center of Crus IIa, on the mediolateral axis of the pfs, and PC dendritic trees traverse most of the width of the crown of Crus IIa. Therefore it is essentially certain that pfs originating in the activated region of the granule cell layer traversed through the postdrug-excited PCs.

Second, there is no other known pathway that would produce this type of excitatory response in PCs. Climbing fibers, for example, are activated by tactile stimuli at much longer latencies (20–35 ms; Brown and Bower 2001, 2002). Whereas our single-unit recordings also would have revealed the complex spike response of the climbing fiber, this input originates outside the cerebellum and there is thus no reason why topically applied bicuculline or gabazine would affect their responses. The only other possible synaptic mechanism for inducing short-latency excitatory responses would require a change in the spatial pattern of granule cell activity in response to peripheral stimulation after drug application. If such a change occurred, then the uncovered responses could result from ascending granule cell input, and not from the pfs. However, we explicitly controlled for this possibility by showing that the granule cell layer both nearby and beneath the recorded PCs is not activated by the stimulus either before or after $GABA_A$ receptors are blocked. This finding is also consistent with previous experiments demonstrating that even peripheral lesions do not result in an unmasking of new receptive fields within these regions of the granule cell layer (Shumway et al. 1999).

In addition to these exclusory arguments, using either of the $GABA_A$-receptor–blocking drugs and two different calculation methods the values of pf conduction velocities are similar and consistent with previous reports in the literature. This is true whether the estimate is based either on the mediolateral distance from the recorded PC to the largest recorded granule cell

layer response to the stimulus or by compared response latencies in two simultaneously recorded PCs.

Finally, the timing and shape of the uncovered responses are also consistent with a direct effect of the pfs. Specially, these responses are generally of lower amplitude and longer duration that those found immediately above activated regions of the granule cell layer. First, this difference is consistent with the fact that pf synapses are less synchronized than the ascending segment synapses converging on overlying PCs. Second, it is likely that fewer pf synapses are activated on each PC from a distant focal excitation than are activated by ascending segment synapses on PCs overlying an activated region of the granule cell layer. Ekerot and Jorntell (2001) estimated that perhaps as few as roughly 2% or 3,000 pf synapses are activated on PCs under these conditions, whereas our electron microscopic studies suggest that a tactile stimulus may activate as many as 25,000 ascending synapses per PC (Gundappa-Sulur et al. 2000). It is also important to point out that these experiments were specifically undertaken to test the predictions of a model, in which the uncovered responses are, for certain, a result of the pfs. Thus the model as well stands as evidence that the uncovered responses are attributed to the pfs.

Functional implications

CONTEXT FOR THESE STUDIES. Most theories of cerebellar cortical function continue to assume that pfs are the primary influence on PC somatic output (Albus 1971; Anastasio 2001; Barto et al. 1999; Bernard and Axelrad 1991; Braitenberg and Atwood 1958; Daya and Chauvet 1999; Hofstotter 2002; Marr 1969; Medina and Mauk 2000; Schweighofer et al. 1998; Yamamoto 2002), even though there is considerable experimental evidence that this is not the case. Although numerous experiments demonstrated that direct electrical molecular layer stimulation of the pfs can produce beamlike responses (Coutinho et al. 2004; Dunbar et al. 2004; Eccles et al. 1966b; Gao et al. 2003; Ito and Kano 1982), almost all efforts to obtain beams of PCs under more natural stimulus conditions have failed. For example, Bell and Grimm (1969) reported a lack of pf-induced correlative firing in PCs separated by more than a few tens of microns, a result also recently reported by Jaeger (2003). Eccles and colleagues found patches—not beams—of activated PCs in the cat cerebellum after peripheral tactile stimulation (Eccles et al. 1972). Our own tactile stimulation mapping experiments found activated PCs only immediately overlying activated regions of the granule cell layer in the rat (Bower and Woolston 1983; Lu et al. 2005), a result also subsequently demonstrated in the cat (Kolb et al. 1997) and the isolated guinea pig cerebellum (Cohen and Yarom 1998). In fact, in the last 50 years, we are aware of only one paper, purported to demonstrate beamlike effects in vivo using direct mapping techniques (Garwicz and Andersson 1992), attributed the previous reports of a lack of PC beamlike responses to possible experimentally induced damage to pfs. However, our present results show that tactile stimuli delivered under exactly the same experimental conditions as those in previous studies (Bower and Woolston 1983) are fully capable of producing excitatory PC beams as long as inhibition is blocked.

Unfortunately, Garwicz and Andersson (1992) and several more recent in vitro studies (Coutinho et al. 2004; Diez-Garcia et al. 2005; Heck 1999; Vranesic et al. 1994), questioning previous in vivo reports of a lack of pf-induced PC beams, also made the assumption that the presence of field potential responses or dendritic currents directly implies a pf excitatory effect on PC somatic firing. The membrane current records from the model shown in Fig. 9 clearly predict that pf volleys can generate substantial dendritic currents without any direct influence on PC somatic spiking. This prediction is also consistent with recent studies showing that pf-induced local field potentials do not change substantially with topically applied GABA-receptor blockers (Caesar et al. 2003). Accordingly, caution must be advised in interpreting field potential data with respect to PC spiking output.

The only other report we are aware of that claims to show direct pf effects on PC output with tactile stimulation in vivo is based on pooled data obtained in different animals and different experiments (Ekerot and Jorntell 2001, 2003). Further, the interpretation of the pooled data relies on the assumption that the "zonal" organization of the cat intermediate cortex is invariant from individual to individual. Although our own previous micromapping studies of tactile projection maps in comparable regions of the rat cortex did show that the general features of the mapping of the body surface in cerebellar tactile maps are conserved from animal to animal (Bower and Kassel 1990), we also showed that there are variations between individuals that could confound the interpretation of pooled data. Therefore although the data they discuss were obtained using single-unit PC recordings and natural peripheral stimulation, their conclusions are not based on a direct comparison of granule cell layer and PC responses within the same subjects.

PF EXCITATORY EFFECTS ARE BALANCED BY MOLECULAR LAYER INHIBITION. The major prediction of our model is that pf excitatory inputs are counterbalanced by inhibitory inputs despite the additional synaptic delays inherent in a feedforward inhibitory pathway. Consistent with this model-based prediction, several recent physiological studies demonstrated that molecular layer interneurons are electrically compact with very large input resistances (Hausser and Clark 1997), resulting in the rapid generation of outputs in response to pf inputs (Carter and Regehr 2002; Chavas and Marty 2003; Clark and Cull-Candy 2002; Suter and Jaeger 2004) and, accordingly, rapid onset of inhibitory postsynaptic currents in PCs (Mittmann et al. 2005).

The inability of pf inputs alone to drive PC spiking output under natural patterns of network activation suggests that they also do not produce classical summing to threshold-type postsynaptic responses (see also Jaeger and Bower 1999; Santamaria and Bower 2005; Santamaria et al. 2002). The recently reported summing effect of granule cell excitation on PCs in an in vitro preparation (Mittmann et al. 2005) shows summing restricted to the first 2 ms after stimulus onset, which our model suggests is the period of time dominated by input from ascending segment synapses in vivo. In another recent in vitro study, Barbour and colleagues showed a small linear summing of pf responses in a preparation that specifically isolated the synaptic effects of pfs from those of the ascending granule cell axon segment (Brunel et al. 2004). However, even relatively large and artificially abrupt direct electrical stimulation of the granule cell layer generated only small summed responses in PCs with no evidence for the generation of

somatic action potentials. In support of the general results presented here both Brunel et al. (2004) and Mittmann et al. (2005) reported that excitatory responses were powerfully restricted in amplitude and duration by molecular layer inhibition.

The importance of inhibition in regulating pf excitatory effects on PCs also clearly suggests that caution is warranted in interpreting the large number of experimental studies, including perhaps especially those looking at long-term depression (LTD), that use inhibitory blocking agents while studying the excitatory effects of pfs on PCs. As shown by our model-based analysis of the timing of onset of different conductances, blocking inhibition essentially allows pf inputs to evoke a cascade of conductance changes that we predict are normally evoked in vivo only by ascending granule cell axon segment synaptic input (Jaeger and Bower 1994). This effect may account for reports of similar amplitude responses evoked by ascending and pf synapses in vitro when inhibition is blocked (Isope and Barbour 2002).

Our models show that synaptic interactions in the PC dendrite can be interpreted only in the context of this cell's large intrinsic voltage-dependent conductances. As such, the interaction of pf and molecular layer interneuron synaptic inputs on somatic spiking is mediated through the large intrinsic Ca and Kca dendritic conductances, which also counterbalance each other's influence on the excitability of the PC dendrite (Jaeger et al. 1997), bearing no resemblance to classical integrate-and-fire neuronal models.

BASKET- AND STELLATE-TYPE INHIBITIONS PLAY DIFFERENT ROLES. On a more specific level, our modeling results make the prediction that the influence of basket- and stellate-type inhibitions on PCs may differ along the course of the pfs. Although basket-type inhibition may be specifically organized to limit the direct influence of pfs on PCs overlying as well as near activated regions of the granule cell layer, stellate-type synapses have a stronger influence at longer distances from the site of granule cell layer stimulation. The spatial changes in the degree of influence of these two types of inhibitory synapses are predicted to be smooth and regular.

Several anatomical features of the cerebellar cortical circuit seem to be consistent with the idea that basket-type inhibition is activated rapidly after local activation of the granule cell layer. First, the dendrites of molecular layer interneurons forming basket-type connections are located deep in the molecular layer (Sultan and Bower 1998), which may also be the location of the fastest conducting pfs (Vranesic et al. 1994). Second, these deep regions of the molecular layer also contain the largest proportion of ascending branch synapses (Gundappa-Sulur et al. 1999), which make direct contact with molecular layer inhibitory interneurons (Sultan and Bower 1998). The recent suggestion that ascending synapses primarily or exclusively terminate on molecular layer interneurons (Apps and Garwicz 2005) is not supported by either physiological (Jaeger and Bower 1999) or anatomical (Gundappa-Sulur et al. 1999) evidence. Third, deep molecular layer interneurons have restricted receptive fields, similar to those of the mossy fibers terminating below the cell (Ekerot and Jorntell 2003). Blocking inhibition also considerably prolongs the excitatory PC response to local granule cell excitation (Figs. 4–6 and Mittmann et al. 2005). This role for basket-type inhibition is quite different from the traditional view that these synapses contribute to an "off-beam" suppression of PC firing (Dunbar et al. 2004; Eccles et al. 1967; Sultan and Heck 2003).

Finally, there is also physiological evidence supporting the prediction that basket-type inhibition has its effects close to the site of granule cell layer activation. Specifically, the strength and somatic location of basket cell inhibitory input (Bishop 1993) are such that they result in a specific drop in firing rates (Korn and Axelrad 1980). In the experimental data shown here (Figs. 3 and 6) and previously (Bower and Woolston 1983), short-latency reductions in PC firing rates are found only over and near regions of granule cell layer activation. The fact that no clear decrease in firing frequency is seen at greater distances is consistent with the prediction that basket-type inhibition is not strongly activated along the course of the parallel fibers.

INHIBITORY INFLUENCES SCALE WITH DIFFERENT LEVELS OF PF ACTIVATION. One possible interpretation of our results is that some active process regulating inhibition or pf synaptic strength might either block or allow pf-induced PC beams depending on the computational circumstances (Isope and Borbour 2002; Mittmann et al. 2005). Instead, our model suggests that feedforward inhibition, coupled with temporal and spatial dispersion of pf activity, provides a built-in mechanism for dynamically balancing excitatory and inhibitory inputs, thus ensuring—among other things—that pf-induced beams of PCs never occur under natural stimulus conditions. This model prediction is consistent with the balancing reported in recent in vitro studies (Brunel et al. 2004).

Although there is evidence that spiking in molecular layer interneurons can be regulated by network connections between the interneurons themselves (Chavas and Marty 2003), the effects appear to be much weaker than are the effects of feedforward inhibition on PCs (Mittmann et al. 2005). Moreover, analysis of the direct network interactions between interneurons have been interpreted to suggest that any such self-regulation specifically buffers mean firing rates against "external challenges" leading to, in effect, a homeostasis in inhibitory influences (Chavas and Marty 2003). Further, pf-induced excitatory postsynaptic currents on both interneurons and PCs facilitate (Clark and Cull-Candy 2002), suggesting that feedforward inhibition can keep pace with pf excitation even during bursts of activity (Mittmann et al. 2005). It was also recently shown that pf inputs do not specifically regulate the effectiveness of molecular layer inhibition (of the basket-type) on PCs, although climbing fiber input apparently can (Rusakov et al. 2005). Thus pf activity does not appear itself able to overcome or cancel the effectiveness of counterbalancing inhibition.

It was also previously suggested that the lack of PC beams in response to discrete tactile stimulation is a result of an insufficiently large or complex pattern of granule cell layer activation (Braitenberg et al. 1997). These authors posit that the correct pattern of peripheral stimuli would induce a tidal wave of increasingly synchronous pfs pushing PCs over threshold. Although we did not specifically test this hypothesis with our model, we have no evidence to believe that feedforward molecular layer inhibition is not fully capable of compensating for changes in the overall amounts of pf excitation. Our results suggest that the cumulative effects of basket-type inhibition under these conditions alone would be expected to ensure that pfs do not directly drive PC output.

Finally, the idea that pf excitation does not directly drive PC somatic output, but instead works in concert with molecular layer inhibition to regulate the large voltage-dependent conductances in the PC dendrite, also suggests an important reinterpretation for the function of activity-dependent synaptic modification within cerebellar cortical circuitry. In particular, although experimental and traditional theoretical studies of LTD in pf synapses interpret these effects to be associated with Marr–Albus style (Albus 1971; Marr 1969) learning (for review see Oyhama et al. 2003), this interpretation is tied to the idea that changes in pf synaptic strength result directly in changes in PC somatic output. Interpreted in the context of a circuit that depends on a balance between pf excitation and molecular layer inhibition, LTD might instead provide a mechanism to maintain that important balance (Bower 2002; De Schutter 1995) and thus is not a mechanism for classic synaptic learning (Kimura et al. 2005).

In summary, our models and experiments have generated a new interpretation for the physiological organization of cerebellar cortex that is quite different from that embraced by most cerebellar physiologists and theorists (Bower 2002). When granule cells are activated by mossy fiber inputs, their influence on PCs appears to first be felt through the nearly synchronous activation of synapses on the ascending segment of the granule cell axon. The data presented here suggest that this input arrives too rapidly for molecular layer inhibition to counteract the resulting excitatory synaptic drive. In contrast, cerebellar cortical circuitry appears to ensure that pfs never directly drive PC output. Near their point of bifurcation, any excitatory somatic effects of more synchronized pfs can be blocked by basket-type somatic inhibition. As the pf volley travels further from its point of origin, and pf influences become more temporally and spatially diffuse, dendritic stellate-type feedforward inhibition controls pf excitation. Thus the present experiments provide additional evidence at the network level, that granule cell synapses on the ascending and pf segments of its axon should be considered functionally distinct (Bower 2002; Gundappa-Sulur et al. 1999; Simms and Hartell 2005, 2006).

The lack of direct drive by pfs on PC spiking does not mean that the pfs have no function. Instead, our modeling (Jeager et al. 1994; Santamaria et al. 2002) and experimental (Jaeger and Bower 1997) results suggest that the state of activation of the PC's large conductances is under the direct local control of pf excitation and molecular layer inhibition. This local regulation, in turn, substantially affects the electrochemical response of the PC to the excitatory drive from synapses associated with the ascending segment of the granule cell axon (Santamaria et al. 2002; Santamaria and Bower 2005). Computationally, in this way pfs work in concert with molecular layer inhibition to provide a context in which to interpret information projected onto PCs by ascending segment synapses (Bower 2002). Similarly, recent modeling and experimental results on pyramidal cells also suggest that large numbers and perhaps the majority of cerebral cortical excitatory synapses may also be involved in the modulation of dendritic dynamics than in directly driving somatic output (Chance et al. 2002; Rhodes and Llinás 2001). Accordingly, theories with respect to the brain that assume that the primary role of excitatory synapses is to sum the postsynaptic cell to threshold may need to be modified.

ACKNOWLEDGMENTS

Present address of F. Santamaria: Dept. of Neurobiology, P.O. Box 3209, Duke University Medical Center (E-mail: santamaria@neuro.duke.edu).

GRANTS

This work was supported by National Science Foundation Grant IBN-0226089 and National Partnership for Advanced Computational Infrastructure.

REFERENCES

Albus JS. A theory of cerebellar function. *Math Biosci* 10: 25–61, 1971.
Anastasio TJ. Input minimization: a model of cerebellar learning without climbing fiber error signals. *Neuroreport* 12: 3825–3831, 2001.
Apps R, Garwicz M. Anatomical and physiological foundations of cerebellar information processing. *Nat Rev Neurosci* 6: 297–311, 2005.
Barto AG, Fagg AH, Sikoff N, Houk JC. A cerebellar model of timing and prediction in the control of reaching. *Neural Comput* 11: 565–594, 1999.
Bell CC, Grimm RJ. Discharge properties of Purkinje cells recorded on single and double microelectrodes. *J Neurophys* 32: 1044–1055, 1969.
Bernard C, Axelrad H. Propagation of parallel fiber volleys in the cerebellar cortex: a computer simulation. *Brain Res* 565: 195–208, 1991.
Bishop GA. An analysis of HRP-filled basket cell axons in the cat's cerebellum. I. Morphology and configuration. *Anat Embryol* (*Berl*) 188: 287–297, 1993.
Bower JM. The organization of cerebellar cortical circuitry revisited: implications for function. *Ann NY Acad Sci* 978: 135–155, 2002.
Bower JM, Beeman D. *The Book of GENESIS*. New York: Springer-Verlag, 1995.
Bower JM, Kassel J. Variability in tactile projection patterns to cerebellar folia Crus IIA of the Norway rat. *J Comp Neurol* 302: 768–778, 1990.
Bower JM, Woolston DC. Congruence of spatial organization of tactile projections to granule cell and Purkinje cell layers of cerebellar hemispheres of the albino rat: vertical organization of cerebellar cortex. *J Neurophysiol* 49: 745–766, 1983.
Braitenberg V, Atwood RP. Morphological observations on the cerebellar cortex. *J Comp Neurol* 109: 1–33, 1958.
Braitenberg V, Heck D, Sultan F. The detection and generation of sequences as a key to cerebellar function: experiments and theory. *Behav Brain Sci* 20: 229–245; discussion 245–277, 1997.
Brown IE, Bower JM. Congruence of mossy fiber and climbing fiber tactile projections in the lateral hemispheres of the rat cerebellum. *J Comp Neurol* 429: 59–70, 2001.
Brown IE, Bower JM. The influence of somatosensory cortex on climbing fiber responses in the rat cerebellum following peripheral tactile stimulation. *J Neurosci* 22: 6819–6829, 2002.
Brunel N, Hakim V, Isope P, Nadal JP, Barbour B. Optimal information storage and the distribution of synaptic weights: perceptron versus Purkinje cell. *Neuron* 43: 745–757, 2004.
Caesar K, Thomsen K, Lauritzen M. Dissociation of spikes, synaptic activity, and activity-dependent increments in rat cerebellar blood flow by tonic synaptic inhibition. *Proc Natl Acad Sci USA* 100: 16000–16005, 2003.
Cajal SR. *La Textura del Sistema Nervioso del Hombre y los Vertebrados*. Madrid: Moya, 1904.
Carter AG, Regehr WG. Quantal events shape cerebellar interneuron firing. *Nat Neurosci* 5: 1309–1318, 2002.
Chadderton P, Margrie TW, Hausser M. Integration of quanta in cerebellar granule cells during sensory processing. *Nature* 428: 856–860, 2004.
Chance FS, Abbott LF, Reyes AD. Gain modulation from background synaptic input. *Neuron* 35: 773–782, 2002.
Chavas J, Marty A. Coexistence of excitatory and inhibitory GABA synapses in the cerebellar interneuron network. *J Neurosci* 23: 2019–2031, 2003.
Clark BA, Cull-Candy SG. Activity-dependent recruitment of extrasynaptic NMDA receptor activation at an AMPA receptor-only synapse. *J Neurosci* 22: 4428–4436, 2002.
Cohen D, Yarom Y. Patches of synchronized activity in the cerebellar cortex evoked by mossy-fiber stimulation: questioning the role of parallel fibers. *Proc Natl Acad Sci USA* 95: 15032–15036, 1998.
Coutinho V, Mutoh H, Knopfel T. Functional topology of the mossy fibre-granule cell–Purkinje cell system revealed by imaging of intrinsic fluorescence in mouse cerebellum. *Eur J Neurosci* 20: 740–748, 2004.
Crepel F, Dhanjal SS, Garthwaite J. Morphological and electrophysiological characteristics of rat cerebellar slices maintained in vitro. *J Physiol* 316: 128–138, 1981.

Daya B, Chauvet GA. On the role of anatomy in learning by the cerebellar cortex. *Math Biosci* 155: 111–138, 1999.

Debarbieux F, Brunton J, Charpak S. Effect of bicuculline on thalamic activity: a direct blockade of IAHP in reticular neurons. *J Neurophysiol* 79: 2911–2918, 1998.

De Schutter E. Cerebellar long-term depression might normalize excitation of Purkinje cells: a hypothesis. *Trends Neurosci* 18: 291–295, 1995.

De Schutter E, Bower JM. An active membrane model of the cerebellar Purkinje cell. I. Simulation of current clamps in slice. *J Neurophysiol* 71: 375–400, 1994a.

De Schutter E, Bower JM. An active membrane model of the cerebellar Purkinje cell. II. Simulation of synaptic responses. *J Neurophysiol* 71: 401–419, 1994b.

De Schutter E, Bower JM. Simulated responses of cerebellar Purkinje cells are independent of the dendritic location of granule cell synaptic inputs. *Proc Natl Acad Sci USA* 91: 4736–4740, 1994c.

Diez-Garcia J, Matsushita S, Mutoh H, Nakai J, Ohkura M, Yokoyama J, Dimitrov D, Knopfel T. Activation of cerebellar parallel fibers monitored in transgenic mice expressing a fluorescent Ca^{2+} indicator protein. *Eur J Neurosci* 22: 627–635, 2005.

Dunbar RL, Chen G, Gao W, Reinert KC, Feddersen R, Ebner TJ. Imaging parallel fiber and climbing fiber responses and their short-term interactions in the mouse cerebellar cortex in vivo. *Neuroscience* 126: 213–227, 2004.

Eccles JC, Llinás R, Sasaki K. Intracellularly recorded responses of the cerebellar Purkinje cells. *Exp Brain Res* 1: 161–183, 1966b.

Eccles JC, Sabah NH, Schmidt RF, Taborikova H. Cutaneous mechanoreceptors influencing impulse discharges in cerebellar cortex. II. In Purkyně cells by mossy fiber input. *Exp Brain Res* 15: 261–277, 1972.

Eccles JC, Sasaki K, Strata P. The profiles of physiological events produced by a parallel fibre volley in the cerebellar cortex. *Exp Brain Res* 2: 18–34, 1966a.

Eccles JC, Sasaki K, Strata P. A comparison of the inhibitory actions of Golgi cells and of basket cells. *Exp Brain Res* 3: 81–94, 1967.

Ekerot CF, Jorntell H. Parallel fiber receptive fields: a key to understanding cerebellar operation and learning. *Cerebellum* 2: 101–109, 2003.

Etzion Y, Grossman Y. Potassium currents modulation of calcium spike firing in dendrites of cerebellar Purkinje cells. *Exp Brain Res* 122: 283–294, 1998.

Gao W, Dunbar RL, Chen G, Reinert KC, Oberdick J, Ebner TJ. Optical imaging of long-term depression in the mouse cerebellar cortex in vivo. *J Neurosci* 23: 1859–1866, 2003.

Garwicz M, Andersson G. Spread of synaptic activity along parallel fibres in cat cerebellar anterior lobe. *Exp Brain Res* 88: 615–622, 1992.

Gundappa-Sulur G, De Schutter E, Bower JM. Ascending granule cell axon: an important component of cerebellar cortical circuitry. *J Comp Neurol* 408: 580–596, 1999.

Hamann M, Rossi DJ, Attwell D. Tonic and spillover inhibition of granule cells control information flow through cerebellar cortex. *Neuron* 33: 625–633, 2002.

Hartmann MJ, Bower JM. Tactile responses in the granule cell layer of cerebellar folium Crus IIa of freely behaving rats. *J Neurosci* 21: 3549–3563, 2001.

Harvey RJ, Napper RM. Quantitative studies on the mammalian cerebellum. *Prog Neurobiol* 36: 437–463, 1991.

Hausser M, Clark BA. Tonic synaptic inhibition modulates neuronal output pattern and spatiotemporal synaptic integration. *Neuron* 19: 665–678, 1997.

Heck D. Sequential stimulation of rat and guinea pig cerebellar granular cells in vitro leads to increasing population activity in parallel fibers. *Neurosci Lett* 263: 137–140, 1999.

Hofstotter C, Mintz M, Verschure PF. The cerebellum in action: a simulation and robotics study. *Eur J Neurosci* 16: 1361–1376, 2002.

Isope P, Barbour B. Properties of unitary granule cell–Purkinje cell synapses in adult rat cerebellar slices. *J Neurosci* 22: 9668–9678, 2002.

Ito M, Kano M. Long-lasting depression of parallel fiber–Purkinje cell transmission induced by conjunctive stimulation of parallel fibers and climbing fibers in the cerebellar cortex. *Neurosci Lett* 33: 253–258, 1982.

Jaeger D. No parallel fiber volleys in the cerebellar cortex: evidence from cross-correlation analysis between Purkinje cells in a computer model and in recordings from anesthetized rats. *J Comput Neurosci* 14: 311–327, 2003.

Jaeger D, Bower JM. Prolonged responses in cerebellar Purkinje cells following activation of the granule cell layer: an intracellular *in vitro* and *in vivo* investigation. *Exp Brain Res* 100: 200–214, 1994.

Jaeger D, Bower JM. Synaptic control of spiking in cerebellar Purkinje cells: dynamic current clamp based on model conductances. *J Neurosci* 19: 6090–6101, 1999.

Jaeger D, De Schutter E, Bower JM. The role of synaptic and voltage-gated currents in the control of Purkinje cell spiking: a modeling study. *J Neurosci* 17: 91–106, 1997.

Kimura T, Sugimori M, Llinás RR. Purkinje cell long-term depression is prevented by T-588, a neuroprotective compound that reduces cytosolic calcium release from intracellular stores. *Proc Natl Acad Sci USA* 102: 17160–17165, 2005.

Kolb FP, Arnold G, Lerch R, Straka H, Buttner-Ennever J. Spatial distribution of field potential profiles in the cat cerebellar cortex evoked by peripheral and central inputs. *Neuroscience* 81: 1155–1181, 1997.

Korn H, Axelrad H. Electrical inhibition of Purkinje cells in the cerebellum of the rat. *Proc Natl Acad Sci USA* 77: 6244–6247, 1980.

Llinás R. Radial connectivity in the cerebellar cortex: a novel view regarding the functional organization of the molecular layer. In: *The Cerebellum: New Vistas*, edited by Plalay S, Chan-Palay C. New York: Elsevier, 1982.

Llinás R, Sugimori M. Electrophysiological properties of in vitro Purkinje cell dendrites in mammalian cerebellar slices. *J Physiol* 305: 197–213, 1980.

Lu H, Hartmann MJ, Bower JM. Correlations between Purkinje cell single unit activity and simultaneously recorded field potentials in the immediately underlying granule cell layer. *J Neurophysiol* 94: 1849–1860, 2005.

Mann-Metzer P, Yarom Y. Electrotonic coupling interacts with intrinsic properties to generate synchronized activity in cerebellar networks of inhibitory interneurons. *J Neurosci* 19: 3293–3306, 1999.

Marr D. A theory of cerebellar cortex. *J Physiol* 202: 437–470, 1969.

Medina JF, Mauk MD. Computer simulation of cerebellar information processing. *Nat Neurosci Suppl* 3: 1205–1211, 2000.

Mittmann W, Koch U, Hausser M. Feed-forward inhibition shapes the spike output of cerebellar Purkinje cells. *J Physiol* 563: 369–378, 2005.

Miyasho T, Takagi H, Suzuki H, Watanabe S, Inoue M, Kudo Y, Miyakawa H. Low-threshold potassium channels and a low-threshold calcium channel regulate Ca^{2+} spike firing in the dendrites of cerebellar Purkinje neurons: a modeling study. *Brain Res* 891: 106–115, 2001.

Morissette J, Bower JM. Contribution of somatosensory cortex to responses in the rat cerebellar granule cell layer following peripheral tactile stimulation. *Exp Brain Res* 109: 240–250, 1994.

Ohyama T, Nores WL, Murphy M, Mauk MD. What the cerebellum computes. *Trends Neurosci* 26: 222–227, 2003.

Pouzat C, Marty A. Somatic recording of GABAergic autoreceptor current in cerebellar stellate and basket cells. *J Neurosci* 19: 1675–1690, 1999.

Rhodes PA, Llinás RR. Apical tuft input efficacy in layer 5 pyramidal cells from rat visual cortex. *J Physiol* 536: 167–187, 2001.

Rusakov DA, Saitow F, Lehre KP, Konishi S. Modulation of presynaptic Ca^{2+} entry by AMPA receptors at individual GABAergic synapses in the cerebellum. *J Neurosci* 25: 4930–4940, 2005.

Santamaria F, Bower JM. Background synaptic activity modulates the response of a modeled Purkinje cell to paired afferent input. *J Neurophysiol* 93: 237–250, 2005.

Santamaria F, Jaeger D, De Schutter E, Bower JM. Modulatory effects of parallel fiber and molecular layer interneuron synaptic activity on Purkinje cell responses to ascending segment input: a modeling study. *J Comput Neurosci* 13: 217–235, 2002.

Schweighofer N, Arbib MA. A model of cerebellar metaplasticity. *Learn Mem* 4: 421–428, 1998.

Shambes GM, Gibson JM, Welker W. Fractured somatotopy in granule cell tactile areas of rat cerebellar hemispheres revealed by micromapping. *Brain Behav Evol* 15: 94–140, 1978.

Shumway C, Morissette J, Gruen P, Bower JM. Plasticity in cerebellar tactile maps in the adult rat. *J Comp Neurol* 413: 583–592, 1999.

Simpson JI, Wylie DR, De Zeeuw CI. On climbing fiber signals and their consequence(s). *Behav Brain Sci* 19: 384–398, 1996.

Sims RE, Hartell NA. Differences in transmission properties and susceptibility to long-term depression reveal functional specialization of ascending axon and parallel fiber synapses to Purkinje cells. *J Neurosci* 25: 3246–3257, 2005.

Sims RE, Hartell NA. Differential susceptibility to synaptic plasticity reveals a functional specialization of ascending axon and parallel fiber synapses to cerebellar Purkinje cells. *J Neurosci* 26: 5153–5159, 2006.

Sonn J, Mayevsky A. Effects of anesthesia on the responses to cortical spreading depression in the rat brain in vivo. *Neurol Res* 28: 206–219, 2006.

Sultan F, Bower JM. Quantitative Golgi study of the rat cerebellar molecular layer interneurons using principal component analysis. *J Comp Neurol* 393: 353–373, 1998.

Sultan F, Heck D. Detection of sequences in the cerebellar cortex: numerical estimate of the possible number of tidal-wave inducing sequences represented. *J Physiol* (*Paris*) 97: 591–600, 2003.

Suter KJ, Jaeger D. Reliable control of spike rate and spike timing by rapid input transients in cerebellar stellate cells. *Neuroscience* 124: 305–317, 2004.

Tahon K, Volny-Luraghi A, De Schutter E. Temporal characteristics of tactile stimuli influence the response profile of cerebellar Golgi cells. *Neurosci Lett* 290: 156–161, 2005.

Van Der Giessen RS, Maxeiner S, French PJ, Willecke K, De Zeeuw CI. Spatiotemporal distribution of Connexin45 in the olivocerebellar system. *J Comp Neurol* 495: 173–184, 2006.

Vranesic I, Iijima T, Ichikawa M, Matsumoto G, Knopfel T. Signal transmission in the parallel fiber–Purkinje cell system visualized by high-resolution imaging. *Proc Natl Acad Sci USA* 91: 13014–13017, 1994.

Watanabe S, Takagi H, Miyasho T, Inoue M, Kirino Y, Kudo Y, Miyakawa H. Differential roles of two types of voltage-gated Ca^{2+} channels in the dendrites of rat cerebellar Purkinje neurons. *Brain Res* 791: 43–55, 1998.

Whittington MA, Traub RD, Kopell N, Ermentrout B, Buhl EH. Inhibition-based rhythms: experimental and mathematical observations on network dynamics. *Int J Psychophysiol* 38: 315–336, 2000.

Womack MD, Khodakhah K. Characterization of large conductance Ca^{2+}-activated K^+ channels in cerebellar Purkinje neurons. *Eur J Neurosci* 16: 1214–1222, 2002.

Wyatt KD, Tanapat P, Wang SS. Speed limits in the cerebellum: constraints from myelinated and unmyelinated parallel fibers. *Eur J Neurosci* 21: 2285–2290, 2005.

Yamamoto K, Kobayashi Y, Takemura A, Kawano K, Kawato M. Computational studies on acquisition and adaptation of ocular following responses based on cerebellar synaptic plasticity. *J Neurophysiol* 87: 1554–1571, 2002.